Metamaterials based on the phase transition of VO_2

Liu Hongwei,[1*] Lu Junpeng[2*], Wang Xiao[3]

[1]Jiangsu Key Lab on Opto-Electronic Technology, School of Physics and Technology, Nanjing Normal University, Nanjing 210023, China

[2]School of Physics, Southeast University, Nanjing 211189, China

[3]Division of Physics & Applied Physics, School of Physical & Mathematical Sciences, Nanyang Technological University, 21 Nanyang Link, Singapore 637371

*phylhw@njnu.edu.cn; phyljp@seu.edu.cn

Abstract

In this article, we present a comprehensive review on recent research progress on design and fabrication of active tunable metamaterials devices based on phase transition of VO_2. Firstly, we provide an introduction regarding mechanisms of metal-to-insulator phase transition (MIPT) in VO_2 investigated by ultrafast THz spectroscopies. By analyzing the THz spectra, the ~~processes~~ evolutions of MIPT in VO_2 induced by different external excitations are described. The superiorities of using VO_2 as building blocks to construct highly tunable metamaterials are discussed. Subsequently, the recent demonstrated metamaterial devices based on VO_2 are reviewed. These metamaterials devices are summarized and described in the categories of working frequency. In each working frequency range, representative metamaterials based on VO_2 with different architectures and functionalities are reviewed and the contributions of the MIPT of VO_2 are emphasized. Finally, we conclude the recent reports and give a prospect on the strategies of developing future tunable metamaterials based onVO_2.

Keywords Metamaterials, vanadium dioxide, phase transition

1. Introduction

Metamaterials have attracted increasing interests in the past two decades because these artificial composite structures have fancifully unconventional properties.[1] Metamaterials are artificial materials with designed sub-wavelength structures including arrays of sub-wavelength wires, split ring resonators (SRRs), fishnet structures, and so forth.[2-4] The designed sub-wavelength structures ~~are designed to~~ couple with the electric or/and magnetic component of the incident electromagnetic waves, which leads to myriad unique phenomena, such as negative refractive index, sub-wavelength focusing and perfect resonant absorption.[5-9] Hence metamaterials provide a platform to explore various applications~~. The demonstrated applications include~~ such as invisibility cloaks,[10, 11] superlens,[12, 13] specific absorbers[14] and strain sensors[15]. However, many applications are impeded due to the lack of tunability and limited working bandwidth, which are mainly determined by the nature of the sub-wavelength structures and the employed materials. Recent reports have demonstrated that different approaches have been used to realize tunable metamaterials devices.[16] These devices possess tunable, switchable or nonlinear response and functionalities.

Tunable metamaterials are known as metamaterials with tunable responses to the incident electromagnetic radiation. The interaction between the tunable metamaterials and the incident radiation can be controlled, thus the response to the

incidence can be actively tuned.[17] In addition, tunable metamaterials allow one to control and manipulate the electromagnetic radiation in a real-time manner. Various approaches have been exploited to facilitate the tunability of metamaterials. Generally, the approaches that are employed to achieve tunable metamaterials can be classified into two major classes. One is based on the reconfiguration of patterned structures, such as bending the substrate,[18-20] reshaping the structure of unit cells,[21, 22] or rotating the unit cell.[23] The other aspect relies on changing the effective electromagnetic properties of substrates [24-29] or the resonators.[30-35] It is facilitated by the flexibility and diversity of the surrounding media or the tunability of the nonlinear properties of the constituent materials. In earlier reports, metamaterials are usually designed to be planar structures composed of arrays of metal patterns with sub-wavelength scale on dielectric substrates.[36, 37] The tunability is realized by controlling the properties (mostly the carrier density) of the substrate rather than the metallic structures. However, the high dielectrics of the substrates restrict the significance of the tunability. To enhance the tunability of metamaterials, two ~~approaches~~ methods based on utilizing functional materials whose property could be significantly tuned upon external excitation have been demonstrated. One ~~approach~~ method is to form hybrid tunable metamaterials,[38-42] where the functional materials ~~is~~ are inserted between the metal resonators and substrate, In the other ~~approach~~method, functional materials replace metals to construct the resonators.[28, 43-46] The tunability of these metamaterials can be achieved by

applying external electrical, thermal and optical controlling.[24, 40, 47-51]

Among these functional materials, phase-change materials are good candidates to provide widely tunable capabilities in metamaterials. The properties of phase-change materials can be tuned in real-time during the structural phase transition process. By using phase-change materials, optical responses of the metamaterials can be significantly modulated by external excitations. VO_2 is a typical phase-change material. ~~classical transition metal dioxide. It is also a famous phase-change material.~~ It exhibits reversible MIPT at about 68 °C. The conductivity presents a change of five orders in magnitude upon the phase transition. The fundamental physics during the transition process has been intensively studied.[52-55] Liu and co-workers studied the ultrafast dynamic behavior of photoinduced MIPT in VO_2 thin films,[56] and investigated the contribution of the size and oxygen stoichiometry to the MIPT behavior of VO_2.[57, 58] The MIPT of VO_2 can be flexibly triggered by ~~the approaches of~~ applying heat, light, electric field, or even direct electrons.[59] This makes VO_2 a promising phase-change material to be utilized ~~to enable~~in tunable metamaterials. By designing different dimensional sub-wavelength structures, VO_2 have been employed to fabricate tunable metamaterials working at THz and other optical frequencies.[29, 47, 48, 60-64] To emphasize the contributions of VO_2 on fabrication of tunable metamaterials, we herein provide a comprehensive overview on the recent related reports. We firstly review the recent investigations regarding fundamental physics of MIPT in VO_2 studied by utilizing ultrafast THz

spectroscopies. The mechanisms of MIPT in VO_2 induced by different stimuli could be clarified *via* the analysis of the THz spectra. We also discussed the superiorities of using VO_2 to form highly tunable metamaterials. Subsequently, we review the recent demonstrated ~~metamaterials~~ metamaterial devices based on VO_2. These metamaterials are summarized and described in the categories of working frequency. Metamaterials based on VO_2 for THz, microwave, infrared and visible spectral ranges are respectively depicted. In each working frequency range, state-of-the-art applications of ~~metamaterials~~ metamaterial devices based on VO_2 are discussed. Finally, we conclude the review and propose prospects on the strategies of developing future tunable metamaterials based onVO_2.

2. Investigations of the MIPT in VO_2 *via* THz spectroscopies

The phase transition of VO_2 is accompanied not only by a significant change of electrical conductivity but also by a remarkable modification of optical absorbance. VO_2 is transparent over the infrared frequency range at insulator phase, while the metallic phase of VO_2 is opaque at most spectral frequencies. Due to its low photon energy, THz radiation is sensitive to the change of free carrier density in phase transition process. Using THz as probe, THz spectroscopies can be employed to clarify the generation of metallic state by directly observing the dynamics of free carrier. The mid-IR or visible light is incapable to identify the existence of metallic domains because the higher photon energy of mid-IR and visible light may excite extra disturbances, such as transient

vibrational modes and the interband excitations. Therefore, THz spectroscopies are befitting techniques to investigate the mechanisms of MIPT in VO_2. In this section, investigations of heating and optical induced MIPT in VO_2 *via* THz spectroscopies are discussed and physical insight into the nature of the MIPT in VO_2 is provided.

2.1 Heating induced transition

VO_2 undergoes a phase transition at a temperature of ~ 68 °C. With the change of temperature, two kinds of phase transitions occur. They are the electronic MIPT and the structural monoclinic-to-rutile phase transition, respectively. These two transitions do not always occur simultaneously.[65-67] Associated with these transitions, dramatic changes of the optical properties at all wavelengths also occur during the phase transition. THz time-domain spectroscopy (THz-TDS) has been employed to study the THz transmission and conductivity of VO_2 with temperature ramping across the phase transition temperature.[68-74] It should be noted that the THz signal only measures the degree of metallization in the phase transition process, while it does not give any information directly regarding the structural change. The transmitted time-domain THz signals are measured, as shown in Figure 1(a). The THz transmission and the conductivity (Figure 1(b)) of VO_2 could be extracted from the recorded spectra. The THz transmission significantly decreases when temperature rises across the phase transition temperature, while the extracted conductivity of VO_2 at insulating state is 2-3

orders lower than that of the metallic state. This is observed in the entire measured frequency range. The real part of conductivity as a function of temperature shows a typical hysteresis behavior, as illustrated in Figure 1(c). The complex conductivity of VO_2 at different temperature is calculated (Figure 1(d)), where the spectra can be described well using Drude-Smith model, given by $\Delta\sigma(\omega)=\frac{\varepsilon_0\omega_p^2\tau_0}{1-i\omega\tau_0}(1+\frac{c}{1-i\omega\tau_0})$, where the parameter $1\le c\le 0$ describes the extent of carrier localization/backscattering in the materials. *c*=-1 corresponds to fully backscattering and/or carrier localization and *c*=0 corresponds to the Drude model. The Drude-Smith model takes into— account for carrier localization and backscattering. Near the phase transition temperature, phase separation and domain formation affect carrier pathways and bring more localization/backscatte~~i~~ring. It should be noted that the measured complex THz conductivity can also be fitted using effective medium theory (EMT) (blue lines in Figure 1(d)). However, the EMT is applicative in some reports,[68, 69, 73] while it does not reproduce the quality of the Drude-Smith fittings in others.[71-73] This discrepancy arises from the differences of the samples, such as the crystalline qualities, grain size and so forth.

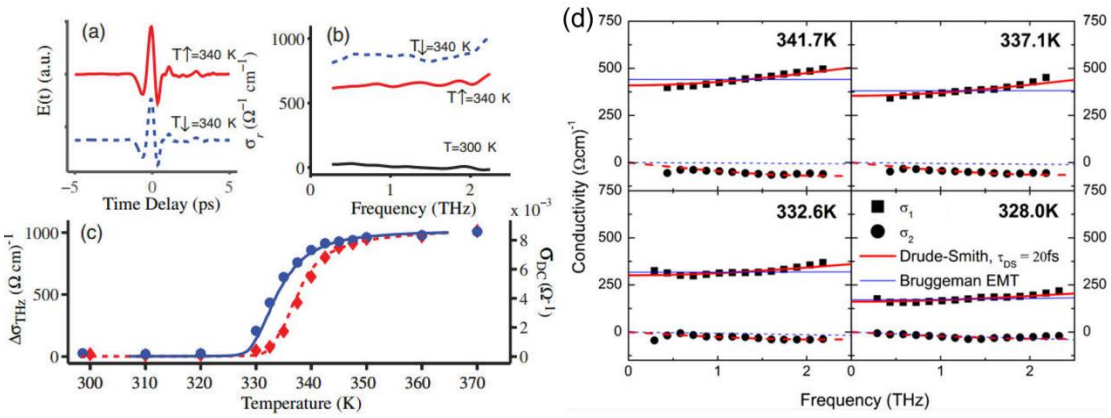

Figure 1. (a) THz waveform transmitted through the sample at 340 K when heated from 300 K (red solid line) and when cooled from 370 K (blue dash line). (b) The frequency-dependent conductivity which determined by the transmitted waveform in (a) and at 300 K. (c) The temperature-dependent hysteresis of THz conductivity (left scale, red diamonds for heating process, blue dots for cooling process) and of the conductance determined by standard dc electrical measurements (right scale, dashed line for heating process, solid line for cooling process). (Reproduced with permission from [74]. Copyright 2007 The American Physical Society) (d) Complex conductivity of VO_2 thin film at different temperatures as the sample is cooled. Red solid lines are best fit of the Drude-Smith model. (Reproduced with permission from [71]. Copyright 2010 American Institute of Physics)

2.2 Optically controlled transition

A photoinduced phase transition of VO_2 can arise in a subpicosecond time scale. This provides an ultrafast method to manipulate the overall phase of the material.[75-77] Optical pump-THz probe (OPTP) spectroscopy has been demonstrated an effective approach to probe the origin of photoinduced phase transition and provide guidance to its potential applications.[56, 57, 74, 78-80] The time-resolved conductivity increases sharply within 1 ps after the photoexcitation, followed by gradually increasing in a time scale of ~100 ps (Figure 2(a)). The sharp increase suggests the formation of metallic phase domains after photoexcitation. The subsequent increase of the conductivity indicates the gradually growth and coalescence of the metallic domains in VO_2

thin film. The maximum conductivity at each pump fluence is extracted (Figure 2(b)) and a nonzero fluence threshold behavior is observed. The existence of a fluence threshold is a well-known feature of the photoinduced phase transition.[57, 74] To further explore the dynamics evolution of the phase transition process, the complex THz conductivity is plotted as a function of pump-probe delay time (Figure 2(c)). The complex conductivity can be well fitted by the Drude-Smith model. By monitoring the temporal evolution of parameter *c*, a clear picture regarding the dynamics of photoinduced phase transition can be obtained. Once the metallic domains are induced in the sea of insulating phase, the backscattering of free carriers occurs at boundaries of the metallic domains. This facilitates a relatively large absolute value of parameter *c*. When metallic domains grow and coalesce to form a continuous film, the domain boundaries reduce and the parameter *c* tends to be zero. Remarkably, if the pump fluence is not sufficient to complete the structural phase transition, the transient metallization can only last a few picoseconds in the THz signal.[79, 81] This phenomenon can be utilized to design metamaterials which requires ultrafast response speed on time scales faster than a nanosecond.

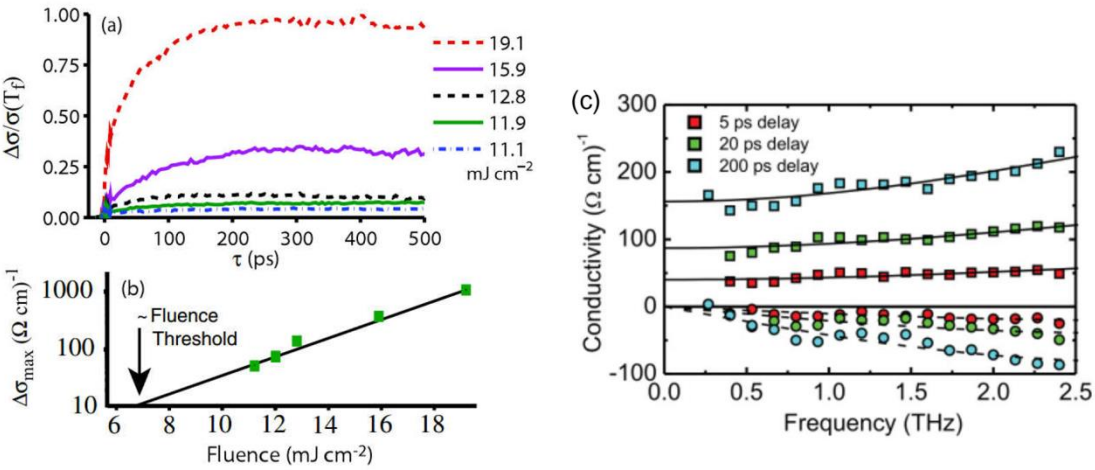

Figure 2. (a) Photoinduced photoconductivity change at 300 K at different fluences ranging from 11.1 mJ/cm^2 to 19.1 mJ/cm^2. (b) Magnitude of conductivity change as a function of fluence at 300 K. (Reproduced with permission from [74]. Copyright 2007 The American Physical Society) (c) Real (squares) and imaginary (dots) photoconductivity at 295 K at various pump-probe delay times. Black lines are fits to the Drude-Smith model. (Reproduced with permission from [80]. Copyright 2012 The American Physical Society)

3. THz Metamaterials based on VO_2

Since the THz signal is very sensitive to conductivity, the significant change of the conductivity induced by the phase transition makes VO_2 a usable component of metamaterials. Combining the phase-change functionality with metamaterials is a promising direction which offers high-contrast, electrical/optical-controlled metamaterial devices.[82] Besides VO_2, gallium metal nanoparticles[83] and germanium-antimony-telluride (GST) films[84-87] have been also utilized to fabricate metamaterials. Comparing with other phase-change materials, VO_2 presents a giant change of conductivity upon the phase transition. In addition, response time can be as fast as picoseconds when the phase transition is induced by optical pump. Furthermore, various approaches have been advised to fabricate VO_2, including sol-gel method, sputtering, PLD approaches, and so forth.[88-91]

This makes it easy to be integrated with other conventional materials (e.g. silicon, quartz, sapphire, etc.).

3.1 Metal resonators/VO_2 hybrid THz metamaterials

Effective manipulation of THz electromagnetic field has attracted great attentions in recent years because of its promising potentials in the applications of nondestructive testing, imaging, security checking, and wireless communication.[92-94] As an artificially designed electromagnetic structure, metamaterials provide an effective means to realize the effective manipulation of THz field and hence THz functional devices.[95] However, the functionalities of the devices are significantly restricted by the intrinsic properties of the constituent materials. To solve this issue, hybrid structures consisting of sub-wavelength structures/functional materials/dielectric substrate are proposed to fabricate versatile metamaterials. The MIPT of VO_2 facilitates it a promising functional material to combine with the metal resonators and ~~to~~ construct active THz devices with hybrid structures. Since the phase transition can be easily triggered by temperature, electric field or light, the operation of the corresponding THz devices could be flexibly realized *via* multiple manners. Various THz metamaterials device consisting of metal resonators on VO_2 thin film have been designed and demonstrated.[40, 49, 60, 61, 96-103]

The thermal-active THz nanoantennas could be facilitated based on VO_2. The operation of the device is realized *via* inducing the phase transition of VO_2 by

heating.[61] VO_2 thin film is inserted between a gold layer and sapphire substrate. An ultra-broad-band slot antenna array is fabricated in the gold layer. The architecture of the metamaterial is illustrated in Figure 3(a). At lower temperature, VO_2 thin film is insulator. The THz transmission spectrum passing through the VO_2 film shows an ultra-broad-band covering the spectral range of 0.2-2 THz (Figure 3(b), blue line). At higher temperature, VO_2 thin film converts to metallic phase. THz transmission is dramatically suppressed over the whole frequency range (Figure 3(b), red line), where the extinction ratio reaches 1000 to 1. This nano-resonator-based metamaterial converts itself from transparent to opaque in the THz range with increasing temperature. Benefiting from the MIPT of VO_2, both ultra-broad-band operation and full transmission/extinction control are achieved simultaneously in this hybrid metamaterials device.

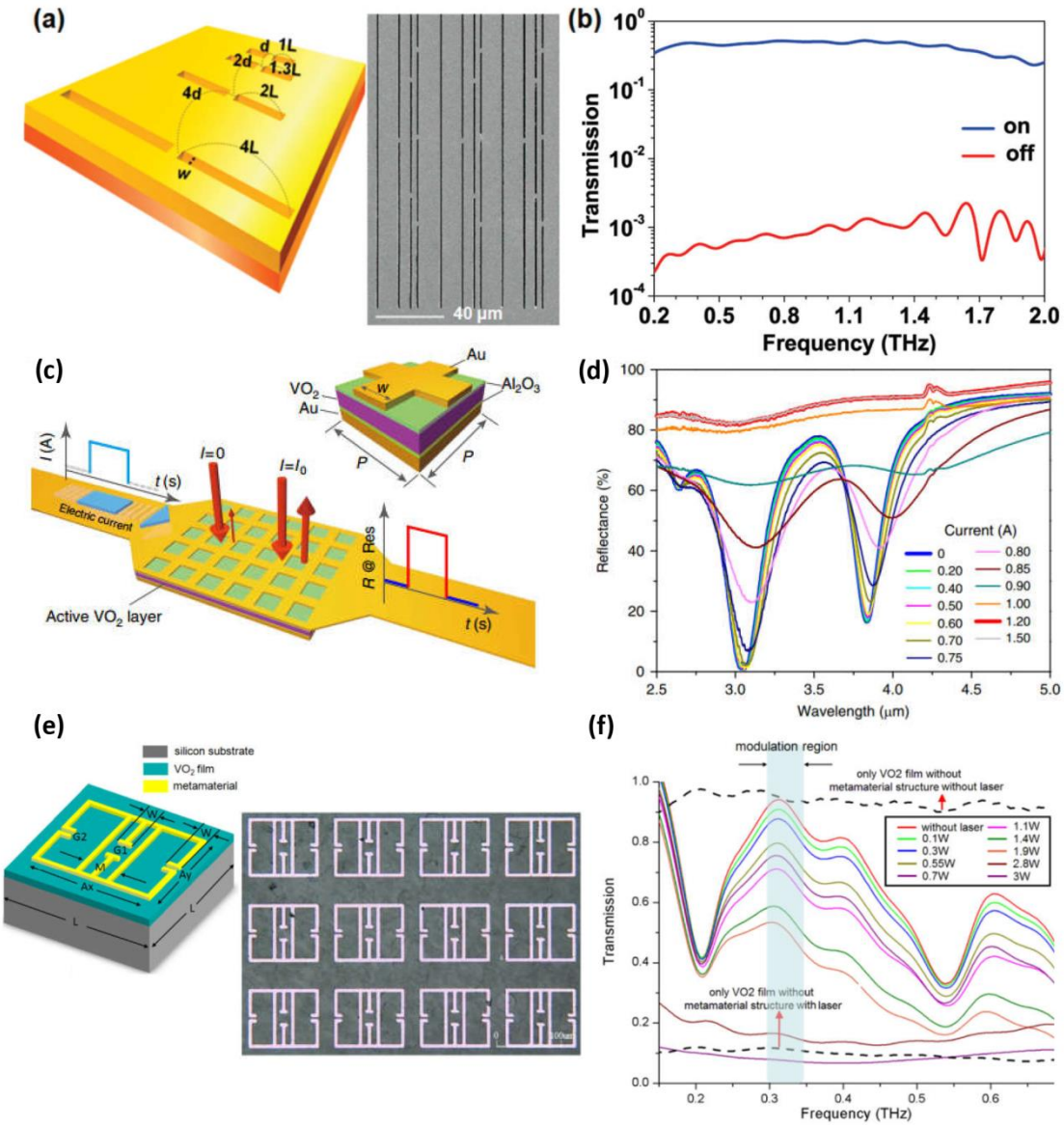

Figure 3. (a) Illustration for ultra-broad-band gold resonator patterns on a VO_2 thin film. (left). SEM image of ~~a~~ the nanoresonator pattern (350 nm width and 50, 60, 100 and 200 μm lengths with 3, 5, 7, 13 μm separations, respectively). (b) Transmittance spectrum of the ultra-broad-band resonator on VO_2 thin film at the frequency ranging from 0.2-2.0 THz at 305 K (blue line) and 375 K (red line). (Reproduced with permission from [61]. Copyright 2010 American Chemical Society) (c) Schematics of the electrical-controlled metamaterials device. Unit cell of the metamaterials absorber is depicted in the inset where P=1550 nm and w=600 nm. The top patterned gold layer is connected to an electric field, which simultaneously supports optical resonances and electrical functionality for Joule heating. The reflectance of incident light can be tuned immediately as a function of the current flowing through the layer, which induces the MIPT in VO_2. (d) Measured reflectance spectra for various intensities of electrical current applied. (Reproduced with permission from [40]. Copyright 2016 Macmillan Publishers Limited) (e) 3D model of a unit cell of the dual-resonance metamaterials-VO_2 hybrid structure. (left) SEM image of the manufactured array. (right) (f) Frequency spectra obtained by THz-TDS. The phase

transition of VO_2 thin film is triggered by an external 808 nm laser with different pump power. (Reproduced with permission from [98]. Copyright 2014 Optical Society of America)

Besides the thermal-active manner, an electrical-active metamaterial has also been demonstrated based on VO_2.[40] The operation of the device is realized *via* inducing the MIPT of VO_2 by applying electrical field. Figure 3(c) schematically illustrates the architecture of this hybrid metamaterial. It consists of a sandwich structure with a patterned-mesh top gold layer, an active VO_2 thin film and a gold ground plane. Al_2O_3 layers are inserted in between gold and VO_2. The thin Al_2O_3 layer can lower the impact of the loss of VO_2 at room temperature to achieve sharper resonance. In addition, Al_2O_3 layer can serve as a diffusion barrier which promotes the crystallization of VO_2 during the fabrication process.[40] The top gold layer is connected to an external circuit which can provide Joule heat as a result of in-plane current flow. The performance of this electrical-active metamaterial is shown in Figure 3(d). Comparing with the spectrum at I = 0 A, absolute modulation of 80% and 75% can be observed at wavelength of 3.05 and 3.85 μm when I rises to 1.2 A. For the current values between 0 A and 1.2 A, the THz waves are gradually scaled with current. This can be attributed to the percolation progress of VO_2. The percolation progress produces localized phase transformations which change the permittivity of VO_2 and thus affect the response of the metamaterials. In addition to the modulation of the amplitude, the resonance frequencies can also be adjusted (Figure 3(d)). The observed hysteresis behavior is consistent with the MIPT process of VO_2. These results render the metamaterials

based on VO_2 the promising potentials in the multifunctional THz optoelectronics, such as metasurfaces for sensing and imaging,[104-106] switchable nanoantenna arrays,[107-109] and memory structures.[60, 101, 110, 111] By applying a series of electrical current pulses (Figure 3(d)), the electrical switching effect was demonstrated. Besides the significant variation of the conductivity during MIPT, the characteristic curves of VO_2 also exhibit hysteresis. Taking advantage of this hysteric behavior, memory effects in metamaterials are realized. By controlling the metallic and insulator state of VO_2, the switch of '0' and '1' states can be flexibly achieved.

Photoinduced active THz functional devices with the combination of dual-resonance metamaterial and VO_2 film have been recently demonstrated.[98] The design of the dual-resonance metamaterial is shown in Figure 3(e). The transmittance of the THz wave through the device could be effectively modulated by the external pump laser (Figure 3(f)). The modulation depth reaches the maximum at the well-transmission frequency band of 0.28-0.36 THz. This region is defined as "modulation region". This device could provide an ultrafast modulation speed of 1 MHz under the control of the pump laser. The photoinduced characteristics of this device may have potential applications in THz functional components, including modulators, intelligent switches, sensors and other devices of interest.

Considering the described results above, metamaterials can significantly promote the development of THz technology. Vice versa, THz technology can enhance our

understanding of the interaction between metamaterials and electromagnetic waves.[64, 103] A representative example is the observation of metamaterials-enhanced high-field THz pulses.[64] In this work, the THz electrical field in the SRR capacitive gap can be significantly enhanced by more than one order of magnitude. Figure 4(a) shows the optical image of a SRR structure deposited on VO_2 thin film. Full wave electromagnetic simulations are commonly employed to reveal the features of the field enhancement in SRRs. The simulated transmission spectrum in the middle of the horizontal gaps presents a broadband enhancement of the THz field (Figure 4(b)). Figure 4(c) illustrates the spatial resolution of the field enhancement. The enhancement is more significant in the horizontally gaps, where it shows a 27-fold enhancement of the THz filed. The SRRs are very sensitive to the power of the incident THz fields (Figure 4(d)). At the highest electrical field of 4 MV cm^{-1}, the in-gap enhanced THz field is high enough to cause the permanent damage of the VO_2 metamaterials. The damage of VO_2 thin film can be observed by SEM image (Figure 4(e)). Moreover, the enhanced THz field can induce phase transition of VO_2 thin film. The phase transition of VO_2 can be confirmed by THz pump-probe measurement which monitors time-resolved transmission of a weak-field THz probe. This work has demonstrated that metamaterials can be used to enhance THz pulse and the enhanced THz field can induce phase transition of VO_2. Methodology in this work can be used to study THz-induced phase transition in other materials.

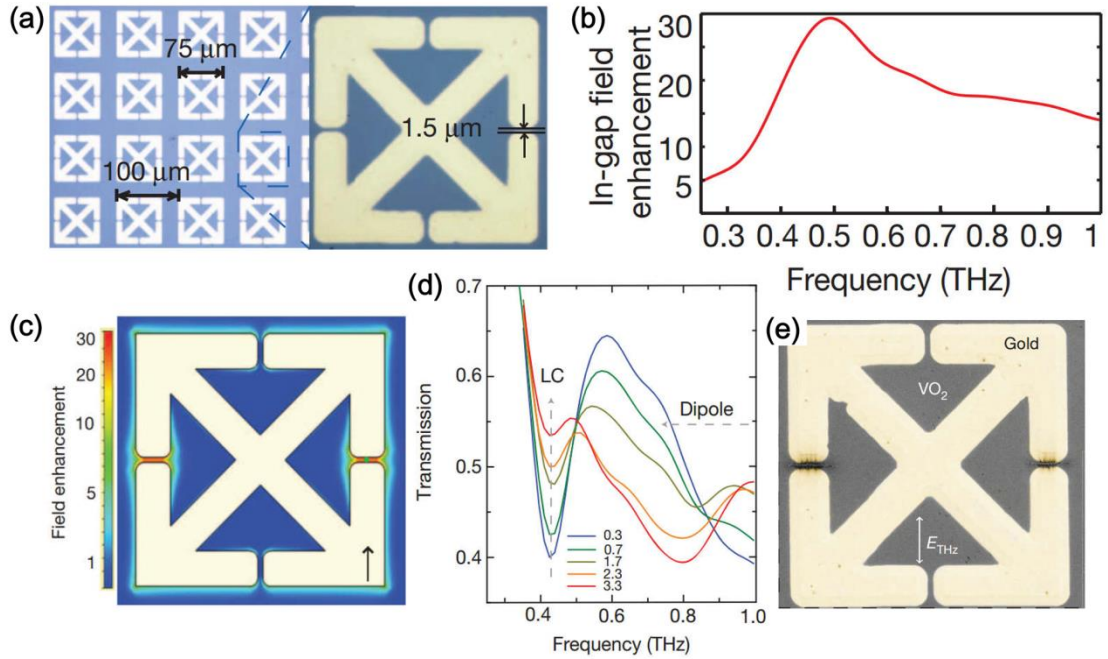

Figure 4. (a) Optical image of metamaterial SRRs deposited on VO_2/sapphire. The SRR gap is 1.5 μm. (b) Frequency-dependent in-gap electric field enhancement. (c) Simulations of the electric field enhancement in the SRRs. (d) Field-dependent transmission spectra of SRRs on VO_2 at 324 K, corresponding the in-gap field ranging from 0.3 to 3.3 MV cm^{-1}. (e) THz-field-induced damage of a single SRR as revealed by SEM image. (Reproduced with permission from [64]. Copyright 2012 Macmillan Publishers Limited)

3.2 Active THz metamaterials with VO_2 resonators

Recently, resonators made of semiconductor,[28, 43, 45] ferroelectric materials[44] or phase transition materials[46, 112, 113] have been employed to construct frequency agile metamaterials. However, some of these devices have difficulties in real applications because they need complex operation conditions such as strong applied magnetic field or low temperature. Based on the MIPT of VO_2, the realization of this kind of metal-free metamaterials is greatly promising. A planar metamaterial, whose resonators are VO_2 cut-wires, have been fabricated and operated.[46] SEM image of a THz metamaterial consisting of VO_2 cut-wires resonators on silica glass is shown in Figure 5(a). To achieve strong THz

resonance, the parameters of VO_2 cut-wires are optimized. The measured THz transmission spectra are shown in Figure 5(b), where the modulation of the transmission is achieved by controlling the temperature of the device. High THz transmission over the measured frequency range is observed at 300 K. VO_2 thin film is insulating at that temperature. However, when VO_2 transforms to its metallic state at higher temperature, the THz transmission decreases and a resonant absorption is observed. A resonance around 0.6 THz is observed and the THz transmission drops to 17% at 340 K. Comparing with the transmission at room temperature, large transmission modification over 65% at ~0.6 THz is achieved. The most significant drop of the THz transmission occurs in a narrow temperature window (320-340 K). This window is consistent with the temperature region where the phase transition of VO_2 occurs. The variation of the measured transmission with temperature is consistent with the variation of the simulated transmission with the conductivity of VO_2 (Figure 5(c)). It reveals that the conductivity of VO_2 increases almost ~~2~~ two orders of magnitude in the temperature range of 320-340 K. The modulation speed of this device would be very fast as it is dominated by the speed of the MIPT of VO_2 which is in the time scale of picosecond.

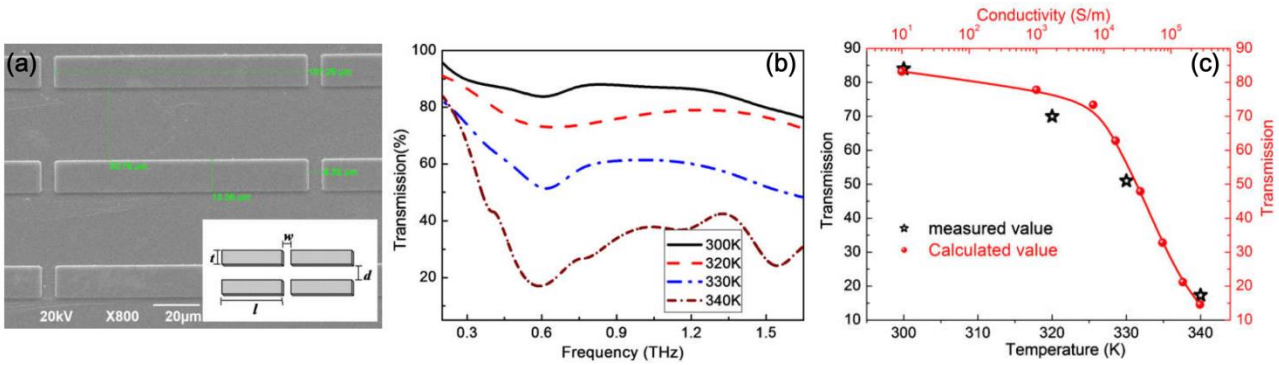

Figure 5. (a) SEM image of the VO_2 cut-wire array. The designed size is as below: *l*=108 μm, *w*=6 μm, *d*=30 μm, and *t*=13.5 μm. Inset displays the schematic of the cut wire structure. (b) Measured THz transmission of VO_2 cut-wire metamaterials at different temperature. (c) Comparison of measured (stars) and simulated (dots) transmission at resonance frequency (0.6 THz). (Reproduced with permission from [46]. Copyright 2010 American Institute of Physics)

4. Metamaterials based on VO_2 for other spectral ranges

Besides the modulation of THz radiation, metamaterials based on VO_2 can also be employed to modulate radiations with other optical frequencies, such as microwave, infrared and visible radiations. In this section, we will review the metamaterials based on VO_2 used for these spectral ranges.

4.1 Microwave spectral range

Metal resonators with larger size would facilitate the metamaterials working at higher frequency region. Besides the THz metamaterials, VO_2 has been employed as the building block of metamaterials working at microwave frequency when metal resonators with larger size are designed.[114] The active microwave metamaterial is realized by incorporating VO_2 thin film beneath copper SRRs (Figure 6(a) and (b)). The modulation of the amplitude and frequency of the resonance absorption of the device can be achieved *via* inducing the phase transition of VO_2 by changing temperature (Figure 6(c)). At room temperature,

two strong absorption peaks at 9.36 GHz and 18.6 GHz are observed. The maximum absorptivities of these two peaks are 87.0% and 93.0%, respectively. When temperature increases to 345 K, the absorptivity of the peak at lower frequency decreases from 87.0% to 71.7%, while the peak position shifts from 9.36 GHz to 9.98 GHz. The maximum absorptivity of the peak at high-frequency presents a dramatic drop from 93.0% to 39.4% and the peak position shifts from 18.6 GHz to 19.1 GHz. Hence a relative amplitude modulation of ~ 57.6% at microwave region (~ 19 GHz) is realized in VO_2-based microwave metamaterials. The remarkable variation of the absorption characteristics only occurs at a narrow temperature window (337 to 345 K, Figure 6(d)). This is consistent with the temperature range of the MIPT of VO_2. Thus it can be concluded that the thermally triggered phase transition of VO_2 facilitates the modulation functionality of the microwave metamaterial.

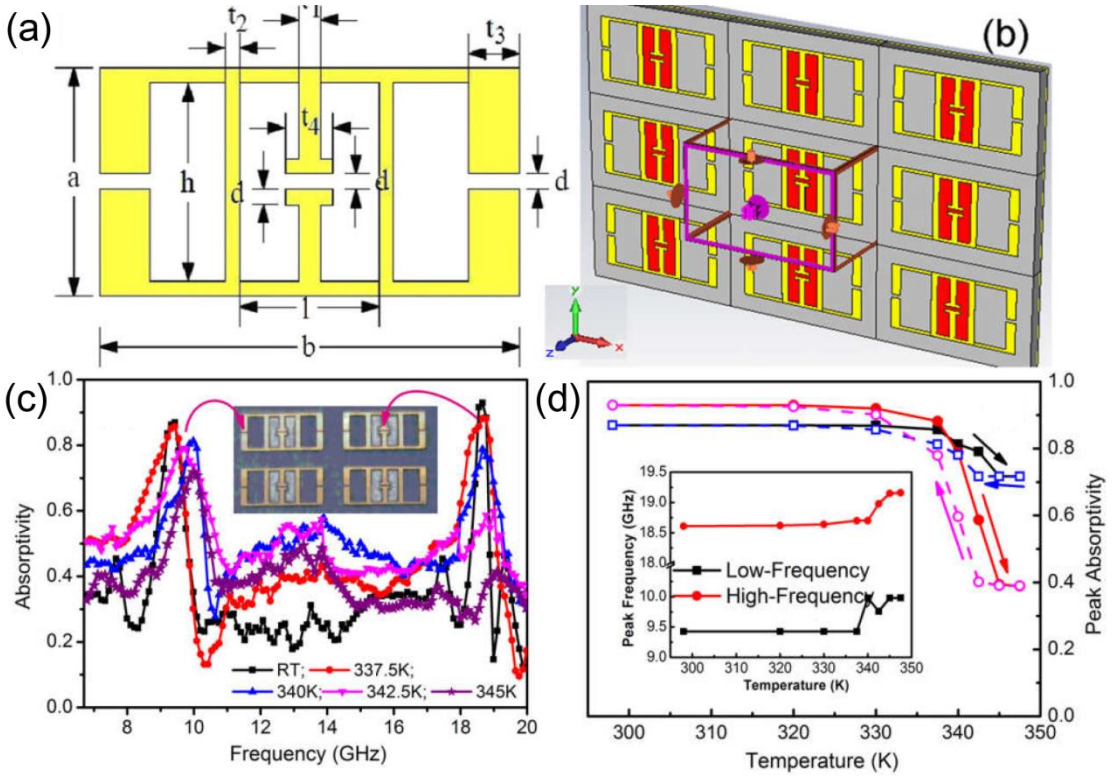

Figure 6. (a) Schematic of the designed SRR unit cell of dual-band metamaterials absorbers. (b) Perspective view of the absorber sheet. Gray, yellow and red colors represent the sapphire substrate, copper metal and VO_2 film, respectively. (c) Measured absorption spectra of the VO_2 metamaterial absorber as a function of device temperature. Inset: image of fabricated device. (d) Peak absorption amplitude as a function of temperature. Inset shows the temperature-dependent corresponding peak frequency. (Reproduced with permission from [114]. Copyright 2012 IOP Publishing Ltd)

4.2 IR spectral range

Utilizing the phase transition of VO_2, metamaterials working in IR range can be achieved by using hybrid structures.[29, 115] An active metamaterials working at near-IR wavelengths has been demonstrated based on silver/VO_2 hybrids.[29] This device consists of planar hybrid silver/VO_2 SRR arrays or self-aligned silver/VO_2 SRR arrays (Figure 7(a)). The SEM images of the fabricated SRR arrays are displayed in Figure 7(b). Two resonance peaks (at 2.1 μm and 3.6 μm) are observed after collecting the reflection of the light from the planar hybrid-SRR

structure at room temperature (Figure 7(c)). These two distinct resonant peaks disappear at 85 °C due to the occurrence of the MIPT of VO_2. In the self-aligned hybrid-SRR arrays, the resonant peak is observed at 2.52 μm. When phase transition occurs, the resonant peak red shifts by $\Delta\lambda$=100 nm to 2.62 μm. This work demonstrates that the resonance of metamaterials can be engineered by using different hybridization mechanisms. Moreover, incorporating VO_2 nanostructures in SRR arrays can achieve better performance of the device.

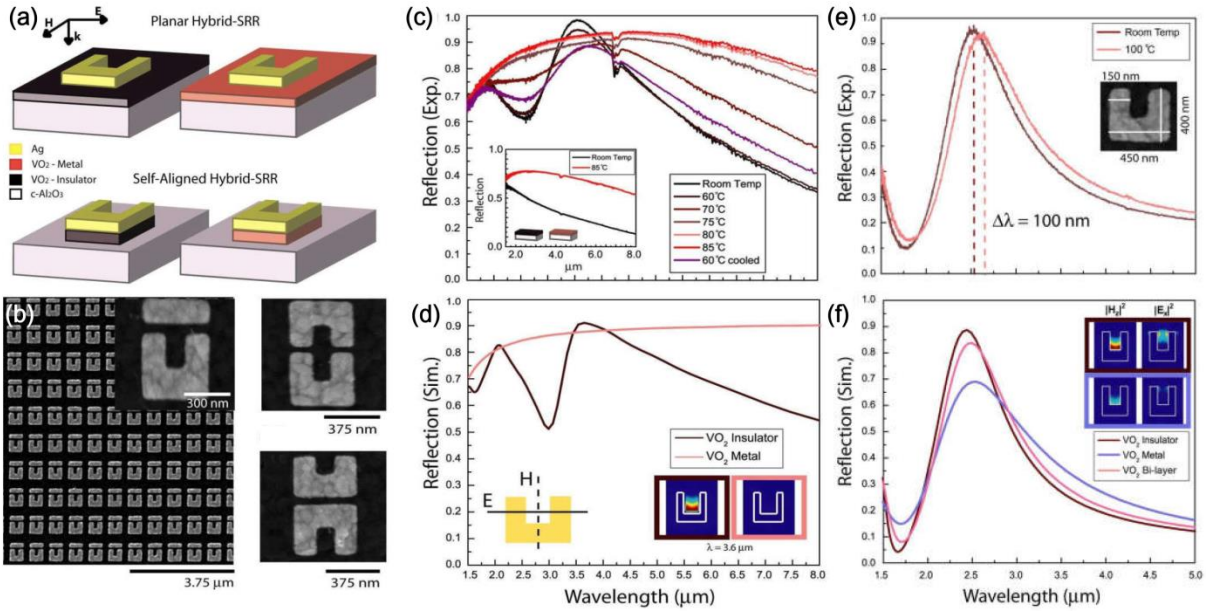

Figure 7. (a) Schematic of a planar hybrid-SRR (top) and a self-aligned (bottom) silver/VO_2 metamaterial unit cell. (b) SEM images of the fabricated coupled-SRR arrays. (c) NIR reflection spectra of 150 nm silver metamaterials arrays on 60 nm VO2 thin films. Inset shows the NIR spectra of a non-pattern VO_2 thin film. (d) Simulated reflect spectra for the same structure using FDTD. (e) NIR reflection spectra of self-aligned 150 nm silver/60 nm VO_2 hybrid-SRR arrays. It shows a 100-nm resonance peak shift. (f) Simulated reflect spectra of the self-aligned hybrid-SRR arrays. (Reproduced with permission from [29]. Copyright 2009 Optical Society of America)

Besides the structure of metal resonators/VO_2 hybrids, the metamaterial only composed of three-dimensional VO_2 nanopillar arrays has been demonstrated to present the working region in IR.[115] The MIPT temperature of VO_2 could be gradually controlled by applying W-doping. The phase transition temperature

gradually decreases with increasing concentration of W in VO_2 (Figure 8(a)). The abrupt change of reflectance across the phase transition is maintained in W-doped VO_2. Figure 8(b) shows the transmittance response of the devices consisting of metallic VO_2 nanopillars with different diameters. The resonance peaks are shifted from 1520 to 1750 nm with increasing diameter from 250 to 460 nm. This is consistent with the results of FDTD simulation (Figure 8(c)). In addition, three-dimensional VO_2 nanopillars consisting of vertical stacks of W-doped VO_2 on undoped VO_2 were further designed. Figure 8(e) and (f) schematically illustrate the architecture of the nanopillar arrays composed of 3% W-doped VO_2 and undoped VO_2.The W-doped VO_2 is metallic while the pristine VO_2 is insulator at room temperature. Thus, a metal-insulator hybrid structure is formed in each pillar. The transmission spectrum presents a broad peak located at ~1900 nm. When the temperature increases beyond the phase transition temperature of undoped VO_2, the upper part of the pillars transforms to its metallic phase. The resonance response of the nanopillars shifts from 1900 to 1750 nm. The shift of the resonance peaks is due to the effective increase of the height of the metallic nanopillars.

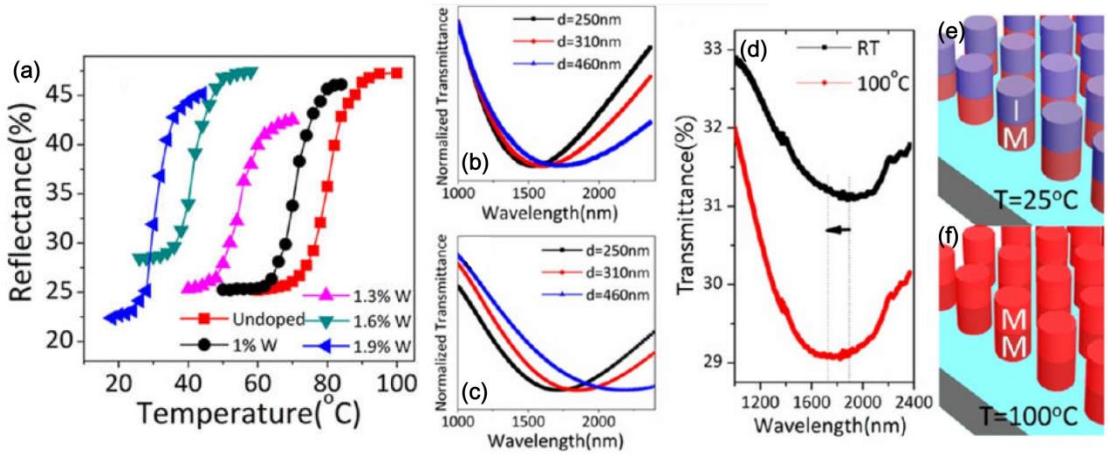

Figure 8. (a) Temperature-dependent reflection of W-doped VO_2 thin films with different W doping concentration at 2500 nm. A decreased phase transition temperature is observed when W doping concentration increases. (b) Experimental and (c) simulated transmittance of VO_2 nanopillar arrays of varying dimensions. (d) Transmittance of layered VO_2 nanopillar arrays which vertically stack with 3% W-doped and undoped VO_2. Schematic of nanopillar arrays at (e) 25 and (f) 100 °C. (Reproduced with permission from [115]. Copyright 2013 American Chemical Society)

4.3 Visible spectral range

A modulator based on VO_2/Au SRRs working in visible spectral range has also been demonstrated.[116] Initially, an Au SRRs with varying gap size on the ITO glass substrate is fabricated. Typical SEM image of the Au SRRs with the gap size of 80 nm is shown in Figure 9(b). The extinction spectra collecting from the samples with different gap sizes (80, 50, 30 nm, respectively) are shown in Figure 9(a). The spectra exhibit two significant resonances. “Peak 1” is due to the coupling of the two arms of SRR and “Peak 2” is attributed to the response of the entire structure. The red shift of Peak 1 in the three samples arises from the decreased interarm distance which enhances the coupling of the two arms and lowers the interaction energy. After depositing 25 nm VO_2 onto the samples, extinction spectra from the SRR/VO_2 hybrids are recorded as a function of

temperature. The resonance position of Peak 1 is extracted from each spectrum and plotted as a function of stabilized temperature (Figure 9(d)-(f)). The resonance peak moves to lower wavelength with increasing temperature. When the sample is cooled down, the peak position returns to its original position. The shift of the resonance arises from the significant decrease of the real part of the permittivity of VO_2 when it transforms to its metallic state.

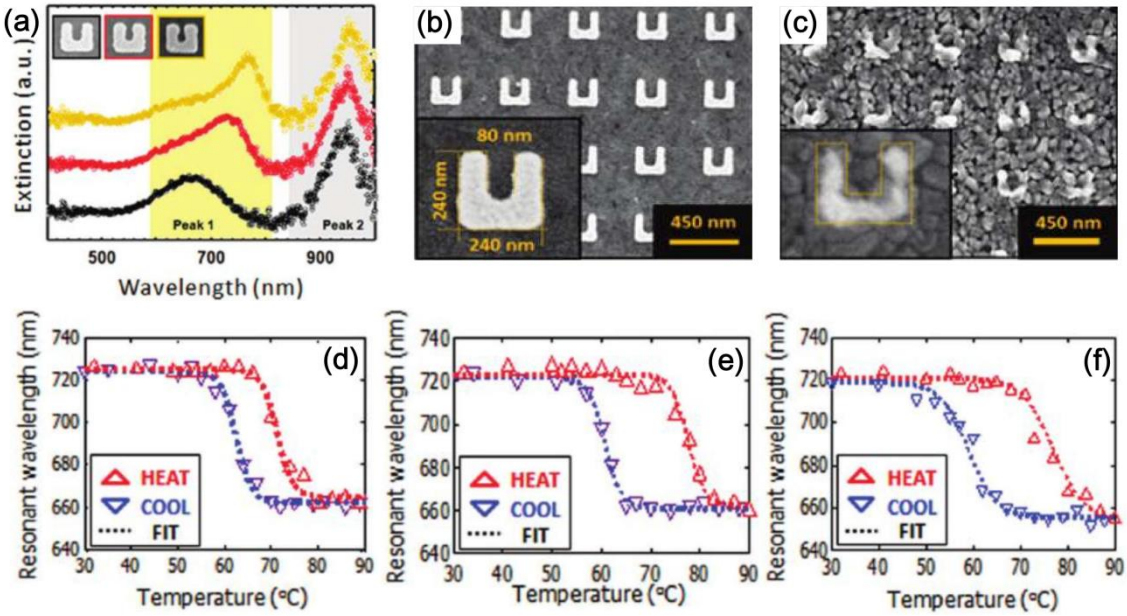

Figure 9. (a) Extinction spectra for the bare Au SRRs with 80 nm gap (black), 50 nm gap (red) and 30 nm gap (yellow), respectively. (b) SEM images of fabricated sample of Au SRRs on ITO substrate. (c) SEM images of a VO_2/Au SRRs sample which is deposited 25 nm VO_2 only. The inset shows the presence of multiple grains within the 80 nm gap. (d-f) Hysteresis diagrams are obtained by monitoring Peak 1 positions of the SRRs with (d) 80 nm, (e) 50 nm and (f) 30 nm gap upon different temperatures. (Reproduced with permission from [116]. Copyright 2011 American Chemical Society)

5. Conclusions and prospects

VO_2 has been demonstrated to present significant and reversible phase transition at relatively lower temperature. This property facilitates VO_2 an effective constituent material to be incorporated into metamaterials. Since the phase

transition could be easily triggered by thermal, electrical or optical approaches, the performance of the tunable metamaterials based on VO_2 could be flexibly controlled by applying heat, light or electric field. In this review, we have provided a comprehensive overview on the recent research efforts to the demonstration of metamaterials based on the MIPT of VO_2. Firstly, we have reviewed the investigations of the MIPT mechanisms in VO_2 *via* THz spectroscopies. Subsequently, we have extended the description to the recent reports on metamaterials devices based on VO_2. THz metamaterial devices consisting of metal resonators/VO_2 hybrid and the metal-free devices consisting of VO_2 resonators are summarized. Metamaterial devices working in other optical frequency ranges, such as microwave, infrared and visible spectral range, are also reviewed. The architectures and functionalities of the metamaterial devices are described and the contribution of the MIPT of VO_2 is emphasized.

Despite varieties of investigations have been reported, further and deeper research efforts are still required to design and fabricate novel metamaterials to realize unique properties. Firstly, there are only few reports on the metamaterials devices whose sub-wavelength structures are made by VO_2. Employing VO_2 as sub-wavelength structures can avoid using noble metal to construct metamaterials. This would reduce the cost of manufacturing. By changing the dimension of the VO_2 resonator, this kind metamaterial is expected to achieve giant modulation depth in a wide frequency range. Secondly, the application of VO_2 to the metamaterials working at visible and near-IR spectral regions is still in the

preliminary stage. The metamaterials working at shorter wavelength regions require the resonators with smaller size. This brings in challenges in the fabrication process. With the development of micro/nano manufacturing techniques, the recent ~~laser~~ laser-based lithography could fabricate nanostructures with sub-wavelength spatial resolution in a high-speed manner.[117, 118] In addition, the micro/nano manufacturing techniques based on electron beam or ion beam have the capacity to fabricate structures with spatial resolution <10 nm over large area substrates with low cost.[119, 120] Recently, Jeong *et al.* fabricated a nanogap-VO_2 hybrid structure.[121] In the 5 nm gap-VO_2 hybrid film structure, the hysteresis behavior can be manipulated *via* nano patterning. The advanced micro/nano manufacturing techniques are expected to promote the realization of multifunctional metamaterials devices working in a wide frequency range.

Considering the reported subpicosecond response time of VO_2 under external stimulus, the VO_2 metamaterial devices may open up new avenues for highly tunable ultrafast metamaterial devices. The ultrafast metamaterial devices can be used in future telecommunication systems. THz communication has been proposed as a promising way to further improve the transmission rate and capacity due to its higher carrier frequency. Although THz communication has many advantages over optical fiber and microwave communications, it has not been widely used due to the lack of mature devices. The realization of novel VO_2 metamaterial devices will allow photonics to compete with electronics in telecommunication systems.

Acknowledgement

This work is supported by “the Fundamental Research Funds for the Central Universities”.

References

[1] Liu Y and Zhang X 2011 Metamaterials: a new frontier of science and technology *Chem. Soc. Rev.* **40** 2494-507

[2] Shelby R A, Smith D R and Schultz S 2001 Experimental Verification of a Negative Index of Refraction *Science* **292** 77-9

[3] Belov P A, Simovski C R and Tretyakov S A 2002 Two-dimensional electromagnetic crystals formed by reactively loaded wires *Phys. Rev. E* **66** 036610

[4] Valentine J, Zhang S, Zentgraf T, Ulin-Avila E, Genov D A, Bartal G and Zhang X 2008 Three-dimensional optical metamaterial with a negative refractive index *Nature* **455** 376-9

[5] Smith D R, Pendry J B and Wiltshire M C K 2004 Metamaterials and Negative Refractive Index *Science* **305** 788-92

[6] Shalaev V M 2007 Optical negative-index metamaterials *Nat. Photonics* **1** 41-8

[7] Zhang X and Liu Z 2008 Superlenses to overcome the diffraction limit *Nat. Mater.* **7** 435-41

[8] Lee J, Lee K, Park H, Kang G, Yu D-H and Kim K 2010 Tunable subwavelength focusing with dispersion-engineered metamaterials in the terahertz regime *Opt. Lett.* **35** 2254-6

[9] Landy N I, Sajuyigbe S, Mock J J, Smith D R and Padilla W J 2008 Perfect Metamaterial Absorber *Phys. Rev. Lett.* **100** 207402

[10] Pendry J B, Schurig D and Smith D R 2006 Controlling Electromagnetic Fields *Science* **312** 1780-2

[11] Cai W, Chettiar U K, Kildishev A V and Shalaev V M 2007 Optical cloaking with metamaterials *Nat. Photonics* **1** 224-7

[12] Smolyaninov I I, Hung Y-J and Davis C C 2007 Magnifying Superlens in the Visible Frequency Range *Science* **315** 1699-701

[13] Liu N, Mesch M, Weiss T, Hentschel M and Giessen H 2010 Infrared Perfect Absorber and Its Application As Plasmonic Sensor *Nano Lett.* **10** 2342-8

[14] Hao J, Wang J, Liu X, Padilla W J, Zhou L and Qiu M 2010 High performance optical absorber based on a plasmonic metamaterial *Appl. Phys. Lett.* **96** 251104

[15] Melik R, Unal E, Perkgoz N K, Puttlitz C and Demir H V 2009 Metamaterial-based wireless strain sensors *Appl. Phys. Lett.* **95** 011106

[16] Boardman A D, Grimalsky V V, Kivshar Y S, Koshevaya S V, Lapine M, Litchinitser N M, Malnev V N, Noginov M, Rapoport Y G and Shalaev V M 2011 Active and tunable metamaterials *Laser Photonics Rev.* **5** 287-307

[17] Chen H-T, Padilla W J, Zide J M O, Gossard A C, Taylor A J and Averitt R D 2006 Active

terahertz metamaterial devices *Nature* **444** 597-600

[18] Tao H, Strikwerda A C, Fan K, Padilla W J, Zhang X and Averitt R D 2009 Reconfigurable Terahertz Metamaterials *Phys. Rev. Lett.* **103** 147401

[19] Khodasevych I E, Shah C M, Sriram S, Bhaskaran M, Withayachumnankul W, Ung B S Y, Lin H, Rowe W S T, Abbott D and Mitchell A 2012 Elastomeric silicone substrates for terahertz fishnet metamaterials *Appl. Phys. Lett.* **100** 061101

[20] Ou J Y, Plum E, Jiang L and Zheludev N I 2011 Reconfigurable Photonic Metamaterials *Nano Lett.* **11** 2142-4

[21] Zhu W M, Liu A Q, Zhang X M, Tsai D P, Bourouina T, Teng J H, Zhang X H, Guo H C, Tanoto H, Mei T, Lo G Q and Kwong D L 2011 Switchable Magnetic Metamaterials Using Micromachining Processes *Adv. Mater.* **23** 1792-6

[22] Fu Y H, Liu A Q, Zhu W M, Zhang X M, Tsai D P, Zhang J B, Mei T, Tao J F, Guo H C, Zhang X H, Teng J H, Zheludev N I, Lo G Q and Kwong D L 2011 A Micromachined Reconfigurable Metamaterial via Reconfiguration of Asymmetric Split-Ring Resonators *Adv. Funct. Mater.* **21** 3589-94

[23] Powell D A, Hannam K, Shadrivov I V and Kivshar Y S 2011 Near-field interaction of twisted split-ring resonators *Phys. Rev. B* **83** 235420

[24] Chen H-T, O'Hara J F, Azad A K, Taylor A J, Averitt R D, Shrekenhamer D B and Padilla W J 2008 Experimental demonstration of frequency-agile terahertz metamaterials *Nat. Photonics* **2** 295-8

[25] Mittleman D 2008 Metamaterials: A tunable terahertz response *Nat. Photonics* **2** 267-8

[26] Werner D H, Kwon D-H, Khoo I-C, Kildishev A V and Shalaev V M 2007 Liquid crystal clad near-infrared metamaterials with tunable negative-zero-positive refractive indices *Opt. Express* **15** 3342-7

[27] Pratibha R, Park K, Smalyukh I I and Park W 2009 Tunable optical metamaterial based on liquid crystal-gold nanosphere composite *Opt. Express* **17** 19459-69

[28] Han J, Lakhtakia A and Qiu C-W 2008 Terahertz metamaterials with semiconductor split-ring resonators for magnetostatic tunability *Opt. Express* **16** 14390-6

[29] Dicken M J, Aydin K, Pryce I M, Sweatlock L A, Boyd E M, Walavalkar S, Ma J and Atwater H A 2009 Frequency tunable near-infrared metamaterials based on VO_2 phase transition *Opt. Express* **17** 18330-9

[30] Kapitanova P V, Maslovski S I, Shadrivov I V, Voroshilov P M, Filonov D S, Belov P A and Kivshar Y S 2011 Controlling split-ring resonators with light *Appl. Phys. Lett.* **99** 251914

[31] Wang Z, Luo Y, Peng L, Huangfu J, Jiang T, Wang D, Chen H and Ran L 2009 Second-harmonic generation and spectrum modulation by an active nonlinear metamaterial *Appl. Phys. Lett.* **94** 134102

[32] Shrekenhamer D, Rout S, Strikwerda A C, Bingham C, Averitt R D, Sonkusale S and Padilla W J 2011 High speed terahertz modulation from metamaterials with embedded high electron mobility transistors *Opt. Express* **19** 9968-75

[33] Shadrivov I V, Kozyrev A B, Weide D W v d and Kivshar Y S 2008 Tunable transmission and harmonic generation in nonlinear metamaterials *Appl. Phys. Lett.* **93** 161903

[34] Gorkunov M and Lapine M 2004 Tuning of a nonlinear metamaterial band gap by an external magnetic field *Phys. Rev. B* **70** 235109

[35] Shadrivov I V, Kozyrev A B, Weide D v d and Kivshar Y S 2008 Nonlinear magnetic

metamaterials *Opt. Express* **16** 20266-71

[36] Hou-Tong C, Antoinette J T and Nanfang Y 2016 A review of metasurfaces: physics and applications *Rep. Prog. Phys.* **79** 076401

[37] Kildishev A V, Boltasseva A and Shalaev V M 2013 Planar Photonics with Metasurfaces *Science* **339** 1232009

[38] Liu P Q, Luxmoore I J, Mikhailov S A, Savostianova N A, Valmorra F, Faist J and Nash G R 2015 Highly tunable hybrid metamaterials employing split-ring resonators strongly coupled to graphene surface plasmons *Nat. Commun.* **6** 8969

[39] Lim C S, Hong M H, Chen Z C, Han N R, Luk'yanchuk B and Chong T C 2010 Hybrid metamaterial design and fabrication for terahertz resonance response enhancement *Opt. Express* **18** 12421-9

[40] Liu L, Kang L, Mayer T S and Werner D H 2016 Hybrid metamaterials for electrically triggered multifunctional control *Nat. Commun.* **7** 13236

[41] Xiong W, Yao J, Li W and Shen J 2013 Hybrid terahertz metamaterial structure formed by assembling a split ring resonator with a metal mesh *Sci. China Phys. Mech.* **56** 882-7

[42] Chen H-T, Palit S, Tyler T, Bingham C M, Zide J M O, O'Hara J F, Smith D R, Gossard A C, Averitt R D, Padilla W J, Jokerst N M and Taylor A J 2008 Hybrid metamaterials enable fast electrical modulation of freely propagating terahertz waves *Appl. Phys. Lett.* **93** 091117

[43] Han J, Lakhtakia A, Tian Z, Lu X and Zhang W 2009 Magnetic and magnetothermal tunabilities of subwavelength-hole arrays in a semiconductor sheet *Opt. Lett.* **34** 1465-7

[44] Němec H, Kužel P, Kadlec F, Kadlec C, Yahiaoui R and Mounaix P 2009 Tunable terahertz metamaterials with negative permeability *Phys. Rev. B* **79** 241108

[45] Han J and Lakhtakia A 2009 Semiconductor split-ring resonators for thermally tunable terahertz metamaterials *J. Mod. Optic.* **56** 554-7

[46] Wen Q-Y, Zhang H-W, Yang Q-H, Xie Y-S, Chen K and Liu Y-L 2010 Terahertz metamaterials with VO_2 cut-wires for thermal tunability *Appl. Phys. Lett.* **97** 021111

[47] Huang W-x, Yin X-g, Huang C-p, Wang Q-j, Miao T-f and Zhu Y-y 2010 Optical switching of a metamaterial by temperature controlling *Appl. Phys. Lett.* **96** 261908

[48] Zhu J, Han J, Tian Z, Gu J, Chen Z and Zhang W 2011 Thermal broadband tunable Terahertz metamaterials *Opt. Commun.* **284** 3129-33

[49] Jeong Y-G, Bernien H, Kyoung J-S, Park H-R, Kim H-S, Choi J-W, Kim B-J, Kim H-T, Ahn K J and Kim D-S 2011 Electrical control of terahertz nano antennas on VO_2 thin film *Opt. Express* **19** 21211-5

[50] Degiron A, Mock J J and Smith D R 2007 Optical Control of Metamaterial Unit Cells at Microwave Frequencies*July 30 2007-Aug. 2 2007)* 10.1109/ISSSE.2007.4294450 p 209-12

[51] Fang X, Tseng M L, Ou J-Y, MacDonald K F, Tsai D P and Zheludev N I 2014 Ultrafast all-optical switching via coherent modulation of metamaterial absorption *Appl. Phys. Lett.* **104** 141102

[52] Yang Z, Ko C and Ramanathan S 2011 Oxide Electronics Utilizing Ultrafast Metal-Insulator Transitions *Ann. Rev. Mater. Res.* **41** 337-67

[53] Budai J D, Hong J, Manley M E, Specht E D, Li C W, Tischler J Z, Abernathy D L, Said A H, Leu B M, Boatner L A, McQueeney R J and Delaire O 2014 Metallization of vanadium dioxide driven by large phonon entropy *Nature* **515** 535-9

[54] Zheng H and Wagner L K 2015 Computation of the Correlated Metal-Insulator Transition in Vanadium Dioxide from First Principles *Phys. Rev. Lett.* **114** 176401

[55] Gray A X, Jeong J, Aetukuri N P, Granitzka P, Chen Z, Kukreja R, Higley D, Chase T, Reid A H, Ohldag H, Marcus M A, Scholl A, Young A T, Doran A, Jenkins C A, Shafer P, Arenholz E, Samant M G, Parkin S S P and Dürr H A 2016 Correlation-Driven Insulator-Metal Transition in Near-Ideal Vanadium Dioxide Films *Phys. Rev. Lett.* **116** 116403

[56] Liu H W, Wong L M, Wang S J, Tang S H and Zhang X H 2012 Ultrafast insulator–metal phase transition in vanadium dioxide studied using optical pump–terahertz probe spectroscopy *J. Phys.: Condens. Matter* **24** 415604

[57] Liu H W, Wong L M, Wang S J, Tang S H and Zhang X H 2013 Effect of oxygen stoichiometry on the insulator-metal phase transition in vanadium oxide thin films studied using optical pump-terahertz probe spectroscopy *Appl. Phys. Lett.* **103** 151908

[58] Hongwei L, Junpeng L, Minrui Z, Hai T S, Haur S C, Xinhai Z and Lin K 2014 Size effects on metal-insulator phase transition in individual vanadium dioxide nanowires *Opt. Express* **22** 30748-55

[59] Mayer B, Schmidt C, Grupp A, Bühler J, Oelmann J, Marvel R E, Haglund R F, Oka T, Brida D, Leitenstorfer A and Pashkin A 2015 Tunneling breakdown of a strongly correlated insulating state in VO_2 induced by intense multiterahertz excitation *Phys. Rev. B* **91** 235113

[60] Driscoll T, Kim H-T, Chae B-G, Kim B-J, Lee Y-W, Jokerst N M, Palit S, Smith D R, Di Ventra M and Basov D N 2009 Memory Metamaterials *Science* **325** 1518-21

[61] Seo M, Kyoung J, Park H, Koo S, Kim H-s, Bernien H, Kim B J, Choe J H, Ahn Y H, Kim H-T, Park N, Park Q H, Ahn K and Kim D-s 2010 Active Terahertz Nanoantennas Based on VO_2 Phase Transition *Nano Lett.* **10** 2064-8

[62] Kats M A, Blanchard R, Zhang S, Genevet P, Ko C, Ramanathan S and Capasso F 2013 Vanadium Dioxide as a Natural Disordered Metamaterial: Perfect Thermal Emission and Large Broadband Negative Differential Thermal Emittance *Phys. Rev. X* **3** 041004

[63] Goldflam M D, Driscoll T, Chapler B, Khatib O, Jokerst N M, Palit S, Smith D R, Kim B-J, Seo G, Kim H-T, Ventra M D and Basov D N 2011 Reconfigurable gradient index using VO_2 memory metamaterials *Appl. Phys. Lett.* **99** 044103

[64] Liu M, Hwang H Y, Tao H, Strikwerda A C, Fan K, Keiser G R, Sternbach A J, West K G, Kittiwatanakul S, Lu J, Wolf S A, Omenetto F G, Zhang X, Nelson K A and Averitt R D 2012 Terahertz-field-induced insulator-to-metal transition in vanadium dioxide metamaterial *Nature* **487** 345-8

[65] Laverock J, Kittiwatanakul S, Zakharov A A, Niu Y R, Chen B, Wolf S A, Lu J W and Smith K E 2014 Direct Observation of Decoupled Structural and Electronic Transitions and an Ambient Pressure Monocliniclike Metallic Phase of VO_2 *Phys. Rev. Lett.* **113** 216402

[66] Nag J, Jr. R F H, Payzant E A and More K L 2012 Non-congruence of thermally driven structural and electronic transitions in VO2 *J. Appl. Phys.* **112** 103532

[67] Tao Z, Han T-R T, Mahanti S D, Duxbury P M, Yuan F, Ruan C-Y, Wang K and Wu J 2012 Decoupling of Structural and Electronic Phase Transitions in VO_2 *Phys. Rev. Lett.* **109** 166406

[68] Jepsen P U, Fischer B M, Thoman A, Helm H, Suh J Y, Lopez R and Haglund R F 2006 Metal-insulator phase transition in a VO_2 thin film observed with terahertz spectroscopy *Phys. Rev. B* **74** 205103

[69] Mandal P, Speck A, Ko C and Ramanathan S 2011 Terahertz spectroscopy studies on epitaxial vanadium dioxide thin films across the metal-insulator transition *Opt. Lett.* **36** 1927-9

[70] Shi Q, Huang W, Zhang Y, Yan J, Zhang Y, Mao M, Zhang Y and Tu M 2011 Giant Phase

Transition Properties at Terahertz Range in VO_2 films Deposited by Sol–Gel Method *ACS Appl. Mater. Inter.* **3** 3523-7

[71] Cocker T L, Titova L V, Fourmaux S, Bandulet H-C, Brassard D, Kieffer J-C, Khakani M A E and Hegmann F A 2010 Terahertz conductivity of the metal-insulator transition in a nanogranular VO_2 film *Appl. Phys. Lett.* **97** 221905

[72] Lourembam J, Srivastava A, La-o-vorakiat C, Rotella H, Venkatesan T and Chia E E M 2015 New Insights into the Diverse Electronic Phases of a Novel Vanadium Dioxide Polymorph: A Terahertz Spectroscopy Study *Sci. Rep.* **5** 9182

[73] Luo Y Y, Su F H, Pan S S, Xu S C, Zhang C, Pan J, Dai J M, Li P and Li G H 2016 Terahertz conductivities of VO_2 thin films grown under different sputtering gas pressures *J. Alloys Compd.* **655** 442-7

[74] Hilton D J, Prasankumar R P, Fourmaux S, Cavalleri A, Brassard D, El Khakani M A, Kieffer J C, Taylor A J and Averitt R D 2007 Enhanced Photosusceptibility near T_c for the Light-Induced Insulator-to-Metal Phase Transition in Vanadium Dioxide *Phys. Rev. Lett.* **99** 226401

[75] Cavalleri A, Tóth C, Siders C W, Squier J A, Ráksi F, Forget P and Kieffer J C 2001 Femtosecond Structural Dynamics in VO_2 during an Ultrafast Solid-Solid Phase Transition *Phys. Rev. Lett.* **87** 237401

[76] Cavalleri A, Rini M and Schoenlein R W 2006 Ultra-Broadband Femtosecond Measurements of the Photo-Induced Phase Transition in VO_2: From the Mid-IR to the Hard X-rays *J. Phys. Soc. Jpn.* **75** 011004-

[77] Dönges S A, Khatib O, O'Callahan B T, Atkin J M, Park J H, Cobden D and Raschke M B 2016 Ultrafast Nanoimaging of the Photoinduced Phase Transition Dynamics in VO_2 *Nano Lett.* **16** 3029-35

[78] Nakajima M, Takubo N, Hiroi Z, Ueda Y and Suemoto T 2008 Photoinduced metallic state in VO_2 proved by the terahertz pump-probe spectroscopy *Appl. Phys. Lett.* **92** 011907

[79] Kübler C, Ehrke H, Huber R, Lopez R, Halabica A, Haglund R F and Leitenstorfer A 2007 Coherent Structural Dynamics and Electronic Correlations during an Ultrafast Insulator-to-Metal Phase Transition in VO_2 *Phys. Rev. Lett.* **99** 116401

[80] Cocker T L, Titova L V, Fourmaux S, Holloway G, Bandulet H C, Brassard D, Kieffer J C, El Khakani M A and Hegmann F A 2012 Phase diagram of the ultrafast photoinduced insulator-metal transition in vanadium dioxide *Phys. Rev. B* **85** 155120

[81] Pashkin A, Kübler C, Ehrke H, Lopez R, Halabica A, Haglund R F, Huber R and Leitenstorfer A 2011 Ultrafast insulator-metal phase transition in VO_2 studied by multiterahertz spectroscopy *Phys. Rev. B* **83** 195120

[82] Zheludev N I and Kivshar Y S 2012 From metamaterials to metadevices *Nat Mater* **11** 917-24

[83] Waters R F, Hobson P A, MacDonald K F and Zheludev N I 2015 Optically switchable photonic metasurfaces *Appl. Phys. Lett.* **107** 081102

[84] Gholipour B, Zhang J, MacDonald K F, Hewak D W and Zheludev N I 2013 An All-Optical, Non-volatile, Bidirectional, Phase-Change Meta-Switch *Adv. Mater.* **25** 3050-4

[85] Chu C H, Tseng M L, Chen J, Wu P C, Chen Y-H, Wang H-C, Chen T-Y, Hsieh W T, Wu H J, Sun G and Tsai D P 2016 Active dielectric metasurface based on phase-change medium *Laser Photonics Rev.* **10** 986-94

[86] Karvounis A, Gholipour B, MacDonald K F and Zheludev N I 2016 All-dielectric phase-change reconfigurable metasurface *Appl. Phys. Lett.* **109** 051103

[87] Yin X, Schäferling M, Michel A-K U, Tittl A, Wuttig M, Taubner T and Giessen H 2015 Active Chiral Plasmonics *Nano Lett.* **15** 4255-60

[88] Kunio O and Naotaka K 2005 Preparation of VO 2 Films with Metal–Insulator Transition on Sapphire and Silicon Substrates by Inductively Coupled Plasma-Assisted Sputtering *JaJAP* **44** L1150

[89] Zhang C, Cao W, Adedeji A V and Elsayed-Ali H E 2014 Preparation and properties of VO2 thin films by a novel sol–gel process *J. Sol-Gel Sci. Technol.* **69** 320-4

[90] Kim D H and Kwok H S 1994 Pulsed laser deposition of VO2 thin films *Appl. Phys. Lett.* **65** 3188-90

[91] Joyeeta N and R. F. Haglund J 2008 Synthesis of vanadium dioxide thin films and nanoparticles *J. Phys.: Condens. Matter* **20** 264016

[92] Tonouchi M 2007 Cutting-edge terahertz technology *Nat. Photonics* **1** 97-105

[93] Ferguson B and Zhang X-C 2002 Materials for terahertz science and technology *Nat. Mater.* **1** 26-33

[94] Siegel P H 2002 Terahertz technology *IEEE T. Microw. Theory* **50** 910-28

[95] Withayachumnankul W and Abbott D 2009 Metamaterials in the Terahertz Regime *IEEE Photonics J.* **1** 99-118

[96] Choi S B, Kyoung J S, Kim H S, Park H R, Park D J, Kim B-J, Ahn Y H, Rotermund F, Kim H-T, Ahn K J and Kim D S 2011 Nanopattern enabled terahertz all-optical switching on vanadium dioxide thin film *Appl. Phys. Lett.* **98** 071105

[97] Hendry E, Lockyear M J, Gómez Rivas J, Kuipers L and Bonn M 2007 Ultrafast optical switching of the THz transmission through metallic subwavelength hole arrays *Phys. Rev. B* **75** 235305

[98] Zhang Y, Qiao S, Sun L, Shi Q W, Huang W, Li L and Yang Z 2014 Photoinduced active terahertz metamaterials with nanostructured vanadium dioxide film deposited by sol-gel method *Opt. Express* **22** 11070-8

[99] Pradhan J K, Anantha Ramakrishna S, Rajeswaran B, Umarji A M, Achanta V G, Agarwal A K and Ghosh A 2017 High contrast switchability of VO_2 based metamaterial absorbers with ITO ground plane *Opt. Express* **25** 9116-21

[100] Lv T T, Li Y X, Ma H F, Zhu Z, Li Z P, Guan C Y, Shi J H, Zhang H and Cui T J 2016 Hybrid metamaterial switching for manipulating chirality based on VO_2 phase transition *Sci. Rep.* **6** 23186

[101] Driscoll T, Palit S, Qazilbash M M, Brehm M, Keilmann F, Chae B-G, Yun S-J, Kim H-T, Cho S Y, Jokerst N M, Smith D R and Basov D N 2008 Dynamic tuning of an infrared hybrid-metamaterial resonance using vanadium dioxide *Appl. Phys. Lett.* **93** 024101

[102] Jun-Hwan S, Kiwon M, Eui Su L, Il-Min L and Kyung Hyun P 2015 Metal-VO_2 hybrid grating structure for a terahertz active switchable linear polarizer *Nanotechnology* **26** 315203

[103] Jun-Hwan S, Kyung Hyun P and Han-Cheol R 2016 Electrically controllable terahertz square-loop metamaterial based on VO_2 thin film *Nanotechnology* **27** 195202

[104] Kats M A, Sharma D, Lin J, Genevet P, Blanchard R, Yang Z, Qazilbash M M, Basov D N, Ramanathan S and Capasso F 2012 Ultra-thin perfect absorber employing a tunable phase change material *Appl. Phys. Lett.* **101** 221101

[105] Rensberg J, Zhang S, Zhou Y, McLeod A S, Schwarz C, Goldflam M, Liu M, Kerbusch J, Nawrodt R, Ramanathan S, Basov D N, Capasso F, Ronning C and Kats M A 2016 Active Optical Metasurfaces Based on Defect-Engineered Phase-Transition Materials *Nano Lett.* **16**

1050-5

[106] Lv T T, Li Y X, Ma H F, Zhu Z, Li Z P, Guan C Y, Shi J H, Zhang H and Cui T J 2016 Hybrid metamaterial switching for manipulating chirality based on VO2 phase transition **6** 23186

[107] Wang D, Zhang L, Gong Y, Jian L, Venkatesan T, Qiu C W and Hong M 2016 Multiband Switchable Terahertz Quarter-Wave Plates via Phase-Change Metasurfaces *IEEE Photonics J.* **8** 1-8

[108] Muskens O L, Bergamini L, Wang Y, Gaskell J M, Zabala N, de Groot C H, Sheel D W and Aizpurua J 2016 Antenna-assisted picosecond control of nanoscale phase transition in vanadium dioxide *Light-Sci. Appl.* **5** e16173

[109] Wang D, Zhang L, Gu Y, Mehmood M Q, Gong Y, Srivastava A, Jian L, Venkatesan T, Qiu C-W and Hong M 2015 Switchable Ultrathin Quarter-wave Plate in Terahertz Using Active Phase-change Metasurface **5** 15020

[110] Driscoll T, Quinn J, Klein S, Kim H T, Kim B J, Pershin Y V, Ventra M D and Basov D N 2010 Memristive adaptive filters *Appl. Phys. Lett.* **97** 093502

[111] Lei D Y, Appavoo K, Ligmajer F, Sonnefraud Y, Haglund R F and Maier S A 2015 Optically-Triggered Nanoscale Memory Effect in a Hybrid Plasmonic-Phase Changing Nanostructure *ACS Photonics* **2** 1306-13

[112] Yan F, Parrott E P J, Humbert G, Crunteanu A and Pickwell-MacPherson E 2015 Switchable terahertz metamaterials: Using the insulator-metal transition of vanadium dioxide to activate metamaterial properties *40th International Conference on Infrared, Millimeter, and Terahertz waves (IRMMW-THz) (Hong Kong, China, 23-28 Aug. 2015)* 10.1109/IRMMW-THz.2015.7327595 p 1-2

[113] Kaltenecker K J, Leroy J, Crunteanu A, Humbert G, Fischer B M and Walther M 2014 THz metamaterials based on metal-insulator transition of VO_2 patterns *39th International Conference on Infrared, Millimeter, and Terahertz waves (IRMMW-THz) (Tucson, AZ, USA, 14-19 Sept. 2014)* 10.1109/IRMMW-THz.2014.6956210 p 1-2

[114] Qi-Ye W, Huai-Wu Z, Qing-Hui Y, Zhi C, Yang L, Yu-Lan J, Yuan L and Pei-Xin Z 2012 A tunable hybrid metamaterial absorber based on vanadium oxide films *J. Phys. D: Appl. Phys.* **45** 235106

[115] Paik T, Hong S-H, Gaulding E A, Caglayan H, Gordon T R, Engheta N, Kagan C R and Murray C B 2014 Solution-Processed Phase-Change VO_2 Metamaterials from Colloidal Vanadium Oxide (VO_x) Nanocrystals *ACS Nano* **8** 797-806

[116] Appavoo K and Haglund R F 2011 Detecting Nanoscale Size Dependence in VO_2 Phase Transition Using a Split-Ring Resonator Metamaterial *Nano Lett.* **11** 1025-31

[117] Malinauskas M, Zukauskas A, Hasegawa S, Hayasaki Y, Mizeikis V, Buividas R and Juodkazis S 2016 Ultrafast laser processing of materials: from science to industry *Light-Sci. Appl.* **5** e16133

[118] Fischer J and Wegener M 2013 Three-dimensional optical laser lithography beyond the diffraction limit *Laser Photonics Rev.* **7** 22-44

[119] Chen Y 2015 Nanofabrication by electron beam lithography and its applications: A review *Microelectron. Eng.* **135** 57-72

[120] Santos A, Deen M J and Marsal L F 2015 Low-cost fabrication technologies for nanostructures: state-of-the-art and potential *Nanotechnology* **26** 042001

[121] Jeong Y-G, Han S, Rhie J, Kyoung J-S, Choi J-W, Park N, Hong S, Kim B-J, Kim H-T and Kim

D-S 2015 A Vanadium Dioxide Metamaterial Disengaged from Insulator-to-Metal Transition *Nano Lett.* **15** 6318-23